

# Assembly and Testing of the ESI Camera DRAFT I

A.I. Sheinis<sup>a</sup>, B. Sutin<sup>c</sup>, H. Epps<sup>b</sup>, J.A. Schier<sup>d</sup>, D. Hilyard<sup>a</sup>, J. Lewis<sup>a</sup>

<sup>a</sup> UCO/Lick Observatory, University of California, Santa Cruz, MS 654, Santa Cruz CA 95064

<sup>b</sup> UCO/Lick Observatory, University of California, Santa Cruz, Kerr Hall, Santa Cruz CA 95064

<sup>c</sup> Carnegie Observatories 813 Santa Barbara Street Pasadena, California 91101

<sup>d</sup> J. Allen Schier Co , 3130 Foothill Blvd., Unit #1, La Crescenta, CA 91214

The Echelle Spectrograph and Imager (ESI), currently being developed for use at the cassegrain focus of the Keck II telescope employs an all spherical, 300 mm focal length F/1 Epps camera. The camera consists of 10 elements in 5 groups; one oil filled doublet, one oil filled triplet, one greased triplet and one singlet and a field flattener mounted in the dewar. Typical mounting tolerances are of order +/- 25 microns. In this paper we discuss the assembly and testing of this camera, along with error budgeting and tolerance analysis.

**Keywords:** spectrograph, imager, echellette, Keck, camera, astronomy

## 1. Introduction:

The Echelle Spectrograph and Imager (ESI) , is a multi purpose spectrograph currently being developed for the cassegrain focus of Keck II telescope by the Instrument Development Lab at Lick Observatory. The instrument is scheduled to see first light in August 29, 1999. ESI is a medium resolution spectrograph, utilizing a fixed 175.6 l/mm echellette grating from Milton Roy (Rochester NY 14625), two large (25 kg) prisms for cross dispersion from Hoya glass (Japan) , polished by Zygo (CT) and coated with a multi-layer dielectric AR at Coherent Inc (Auburn CA). It has three scientific modes: a medium resolution Echelle mode, a low resolution prismatic mode, and a straight imaging mode .

The spectrograph and camera are designed for a wavelength coverage of 0.39 to 1.1 microns. The spectrum is collected by a single 2K x 4k thinned, back-illuminated, MIT-Lincoln Labs CCD chip. The entire spectrum is recorded in a single exposure for both the echellette and low dispersion prism (LD) modes. The echellette mode uses up to a 20 arcsecond long slit and has a resolution  $\lambda/\Delta\lambda$  of approximately 29000 /pixel. The LD mode takes spectra from up to 50 objects or along a single 8 arcminute long slit at a resolution of 1000 /pixel. The imaging mode covers a 2 by 8 arcminute field of view at 0.15 arcseconds per pixel.

The operating temperature range for both the spectrograph and camera are  $-4^{\circ}\text{C}$  to  $+6^{\circ}\text{C}$ . The survivability range is  $-20^{\circ}\text{C}$  to  $+30^{\circ}\text{C}$ .

The camera optical design, shown in figure 1, was performed by one of the authors (H.E.) and consists of four lens groups with ten elements. The effective focal length is 308 mm, has an entrance aperture of 287 mm and a final plate scale of 97.7 microns/arc second on the sky. In the spectrograph the camera operates at about F/2.

The design is all-spherical and includes two large CaF<sub>2</sub> lenses. Group #1 is a doublet, groups #3 and #4 are triplets. The elements in groups #1 and #3 are optically coupled via a fluid (Carguile laser liquid 5610-5000) to minimize internal reflections. The elements in group #4 are greased together with Dow Corning Q2-3067. The last element, a field flattener is mounted in the evacuated CCD dewar and serves as the vacuum window for that dewar.

## 2. Error Budget:

A detailed computer-based sensitivity analysis was performed by one of the authors (B.S.). Individual elements were perturbed axially, radially, or in tilt. The perturbations were 25 microns for axial (Z) and radial (Y) movement, and the tilt (R) was arctangent ( 25 microns / maximum width of the element ) about the center of the element . The perturbed camera model was ray-traced complete with the spectrograph model in echellette mode at 50 different wavelengths, covering all orders, with 1000 rays for each spot. The perturbed system was then compared to the unperturbed system, and the worst centroid change and worst RMS spotsize increase were noted. For the first set of data, no re-focus or active centroiding was done. This calculation corresponds to the worst-case scenario. For the second set of data, the median x-shift and y-shift were subtracted, and a focus correction was estimated and applied. This case corresponds to an active collimator scenario, although the effect of changing spectrograph angle is not included.

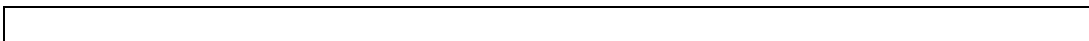
In addition, a similar analysis was performed for the lens groups. Sensitivities were determined by moving entire groups as a solid body and measuring their effect on image size and position.

The following table summarizes this analysis:

(Note: The maximum increase in spot size can be misleading. If a partular image in very good focus, in may be only 0.5 pixels across initially. A defocus of this image would be immeasurable.)

The columns are:

- 1) element number, starting at the first element
- 2) perurbation size (always 25 microns)
- 3) maximum movement of a spot centroid, in microns.
- 4) maximum increase in RMS diameter spot size, in microns.



		no active corrections	active corrections			
element #	Degree of Freedom	Distance ( $\mu$ )	Image motion ( $\mu$ )	Spot size increase ( $\mu$ )	Image motion ( $\mu$ )	Spot size increase ( $\mu$ )
<b>1</b>	Y displacement	25	7.699	0.192	0.185	0.196
<b>1</b>	Z displacement	25	0.219	0.435	0.241	0.035
<b>1</b>	Tip/Tilt	25	10.33	0.509	0.37	0.542
<b>2</b>	Y displacement	25	4.683	0.443	0.185	0.517
<b>2</b>	Z displacement	25	0.087	0.315	0.065	0.01
<b>2</b>	Tip/Tilt	25	12.179	0.132	0.287	0.139
<b>3</b>	Y displacement	25	13.182	1.047	0.722	1
<b>3</b>	Z displacement	25	1.837	3.389	1.721	0.93
<b>3</b>	Tip/Tilt	25	3.678	0.095	0.072	0.052
<b>4</b>	Y displacement	25	13.363	0.277	0.398	0.257
<b>4</b>	Z displacement	25	3.762	4.021	3.672	0.4
<b>4</b>	Tip/Tilt	25	8.747	0.103	0.292	0.117
<b>5</b>	Y displacement	25	1.769	0.221	0.246	0.222
<b>5</b>	Z displacement	25	0.754	0.822	0.736	0.142
<b>5</b>	Tip/Tilt	25	11.166	0.29	0.315	0.299
<b>6</b>	Y displacement	25	4.871	0.267	0.22	0.3
<b>6</b>	Z displacement	25	0.768	0.057	0.773	0.019
<b>6</b>	Tip/Tilt	25	10.12	0.325	0.298	0.268
<b>7</b>	Y displacement	25	4.918	0.02	0.631	0
<b>7</b>	Z displacement	25	0.957	0.326	0.965	0.333
<b>7</b>	Tip/Tilt	25	5.37	0.27	0.56	0.219
<b>8</b>	Y displacement	25	2.411	0.028	0.175	0.014
<b>8</b>	Z displacement	25	2.104	1.276	2.054	0.293
<b>8</b>	Tip/Tilt	25	16.842	0.389	0.246	0.375
<b>9</b>	Y displacement	25	3.298	0.387	0.323	0.407
<b>9</b>	Z displacement	25	3.348	0.979	3.372	0.179
<b>9</b>	Tip/Tilt	25	4.076	0.187	0.742	0.116
<b>10</b>	Y displacement	25	1.016	0.303	0.215	0.291
<b>10</b>	Z displacement	25	2.668	0.963	2.645	0.369
<b>10</b>	Tip/Tilt	25	1.351	0.335	0.461	0.321
<b>1D</b>	Y displacement	25	3.22	0.247	0.128	0.219
<b>1D</b>	Z displacement	25	0.275	0.119	0.276	0.025
<b>1D</b>	Tip/Tilt	25	1.713	0.671	0.219	0.745

<b>1T</b>	Y displacement	25	6.953	0.768	0.164	0.792
<b>1T</b>	Z displacement	25	2.266	3.177	2.158	0.163
<b>1T</b>	Tip/Tilt	25	10.714	0.43	0.285	0.406
<b>2T</b>	Y displacement	25	3.981	0.312	0.403	0.262
<b>2T</b>	Z displacement	25	0.459	2.26	0.558	0.311
<b>2T</b>	Tip/Tilt	25	11.988	0.273	0.051	0.276

These sensitivities were used to create a set of manufacturing tolerances on the mechanical components such that product of the manufacturing and assembly tolerances with the sensitivities produced spot size increases that were small compared with the design spot size. One result of this error analysis was that we decided we couldn't achieve the desired lateral location for cell #2 passively given the current design concept. As a result, we decided to make that degree of freedom adjustable.

In addition, the sensitivity data also allowed us to set a lens motion tolerance in terms of the final image motion allowable for different gravity orientations.

### 3. Camera Optomechanical Design

The optomechanical design was performed by J.A. Schier (JA Schier Co. La Crescenta, CA 9121). The camera mechanical assembly is shown in figure 2 and consists of four cells supported within a single large barrel. The mass of the entire camera assembly is approximately 100 kg. The individual cell assemblies have a mass ranging from 5 to 30 kg. The cells locate radially against lands in the barrel inner wall and axially against athermalizing spacers. Each cell consists of an aluminum cell, radial athermalizing spacers a compressive preload spring. The two oil coupled cells also contain an oil sealing reservoir system. We now describe the five major features of the optomechanical design:

#### Axial Athermalization:

As part of the sensitivity analysis Brian Sutin calculated a linear relationship between the three intergroup spacings, such that the optical impact of small perturbations of one axial distance compensated the perturbations of another axial distance.

Therefore the effective coefficients of thermal expansion (CTE) between the individual groups has been chosen to provide a specific spacing change with temperature to allow the camera to be optically compensated over its operating temperature range. These CTE's were achieved by using a stack of 3 materials, (aluminum, delrin II and polyurethane ) between cell's 2 and 3 and between cells 3 and 4 in order to compensate for a single material (aluminum) between cells one and two.

Actual material CTE's had to be measured in the lab and in some cases differed substantially from

the vendor's catalog quote. In addition, simple material compression had to be considered in the material choice as the weight of the cell + compression spring contributed to a possible compressive force of up to 130 Kg on the spacers.

#### Radial Athermalization:

The purpose of the radial Athermalization is to maintain zero internal stress in all the optical elements over the entire survivability temperature range while maintaining an axial centration below that prescribed by the error budget over the entire operating temperature range.

To achieve this goal, a set of delrin pads were used to match the CTE's of the glass lenses vs the aluminum cells. The pad thickness is varied depending on the CTE of the different glasses. With a diameter clearance of 0.05 mm between the glass and delrin pad all cells have zero thermal induced stresses down to  $-97^{\circ}\text{C}$ . There is no upper bound as the clearance increases with increasing temperature..

An additional factor of great concern is the effect of transient temperature changes. If the ambient temperature cools too rapidly a thermally induced interference can occur within the cells. This is because the aluminum cells have a thermal time constant  $\sim 15$  min while the glass has a thermal time constant  $\sim 120$  minutes. At a temperature difference of  $14^{\circ}\text{C}$  an interference occurs in cell #2, the other cells experience this at a greater temperature difference. With this in mind, we have set  $5^{\circ}\text{C}$  per hour as the maximum transient temperature rate to be experienced by the camera.

#### Cell #2 transverse Adjustment:

As previously noted, cell #2 has the highest sensitivity to translation. One requirement that came out of the error budget process was to have cell #2 adjustable in translation after assembly. This was desired for two reasons: 1) We felt we couldn't achieve the desired lateral location for cell #2 passively, given the current design concept, 2) It was noted that translational adjustment of cell #2 could compensate for other fabrication and assembly errors in the other cells, to some extent.

Figure 3 shows the cell #2 assembly. A 0.5 mm passage has been cut completely through the cell except for three transverse flexures. This cut effectively creates an inner and outer cell. A preload spring is mounted in the outer cell along with two adjuster screw assemblies. This allows the inner cell to be adjusted transversely relative to the outer cell. In this way transverse adjustment of cell #2 is achieved.

#### Optical coupling fluid control:

Cells #1 and #3 contain an optical coupling fluid to minimize internal reflections between elements within the cell. An o-ring seal is provided at the glass aluminum interface. The o-ring is compressed at the minimum nominal dynamic seal specification (8% ???). The o-ring is compressed such that the optic locates directly against the aluminum land and the o-ring carries much of the load while providing a seal.

A heat sealed polyurethane bladder is used to accommodate volumetric changes of the coupling fluid within the cell. We have tested reactivity of the optical coupling fluid against polyurethane and other substances (Hilyard et al, this conference).

## **4.Assembly and Alignment Procedure**

The camera assembly procedure was developed interactively with the aid of a set of “dummy optics” fabricated from aluminum. First the cells are assembled on a precision rotary table. Both the optics and cells are aligned to the rotary table by minimizing their horizontal and vertical runout. Next the optics are held rigidly in place while the cells are jacked into position. Optics retainers with preload springs are then installed onto each assembly. The rest of the mechanicals are then installed onto the cell, including the oil handling system.

The oil is added to the cells via a gravity feed system. The oil has been previously “pumped on’ to remove any dissolved gasses. Initially we had planned to place the filled cells in an evacuated chamber to remove any remaining gas. This was subsequently determined to be unnecessary.

For cells #1, #2, and #3 a hand operated hoist is used to lower the cells into the barrel one at a time. Cell #4 is jacked into place from below. Measurements are made of the “stack height” as the cells are installed to confirm that the cells are seated properly on the spacers.

With the exception of the translational location of cell #2 the camera optical alignment is achieved by close tolerance fabrication of the camera mechanical assembly.

As mentioned previously, lands within the barrel determine the lateral location of the cells. The barrel lands have been final machined in a single lathe operation such that they are concentric to 0.025 mm. They have then been honed individually to match the as-measured isothermal cell diameters, such that the clearance is ~ .025 mm. Shims are added radially in the final assembly to take up this gap.

The radial locating surface within the cells, i.e. the inner diameter on the delrin athermalizing spacers has been final machined to match the as-measured isothermal optic diameters plus a .05 mm assembly clearance. This was done after the spacers were assembled into the cell to increase the centration accuracy of the hole relative to the outer diameter.

Axially, cell #1 locates against the front of the barrel via an internal land. All other cells locate against the back of the barrel through the other cells and associated spacers. Thus cells 2, 3 and 4 along with their

spacers make up a stack whose axial thermal compensation is described above.

After the cells are assembled, the final optical-vertex to cell-land was measured. Only then were the final lengths of the axial spacers cut. This was done to remove as much axial assembly error stack up as possible.

## **5. Camera Bench Testing and Performance analysis**

After final assembly of the camera several optical performance tests were carried out. The results of the tests were then compared to the predictions of the lens design and analysis. We now describe the two fundamental tests.

Interferometric test:

A double pass interferogram was taken of the camera by sending an  $f/0.7$  converging .633 micron beam from a Zygo Mark IV interferometer into the image plane, through the camera and returned off a reference flat. The results of this test were compared to a raytrace on Zemax. These are shown in figure #4.

The results of the interferometric tests compare very consistently with the prediction of the optical design.

Spot size/BFL measurement:

The polychromatic star image was projected through the camera via a projecting telescope. Its size and distance from the last element both on and off axis were inspected via microscope mounted on a five-axis translation stage. This information was digitized via a Cohu video camera and Matrox frame grabber board. The digital information was compared to the design spot sizes via IDL.

On axis we measured the FWHM of the polychromatic spot, through a broad band optical filter, to be 10.6 microns (.7 pixels). This is comparable to the design. The BFL measure was exactly that predicted by the design on the first assembly prior to oil fill. However, the BFL measure was long by 0.2 mm at the final assembly measurement. The most likely candidate for this error has been determined to be the reduction of intra-cell distances in cell #4 due to the leakage of some of the coupling grease in that cell. This issue will be addressed at Keck in August by regreasing the last group before reassembly.

## **7. Conclusion:**

In conclusion, we have described the optomechanical design, assembly and testing of a 10 element, all spherical f/1 Epps camera. The camera is part of the ESI spectrograph, slated to see first light in August of this year. The results of the in-house camera performance testing are encouraging. The proof of the camera performance will be seen in August in Hawaii.

## **8. Acknowledgments**

The authors wish to thank Carol Osborne and Mary Poteete for their help with the design drafting and many of the Figures for this paper. Also, we would like to thank Jerry Nelson, Terry Mast, Matt Radovan and Jack Osborne for their many helpful comments;

## **9. Appendix A: Lens Design performance**

(what goes here???????)

## **9. Bibliography:**

(more to be added!!!!)

- 1) H.Epps and J.Miller, "Echelle Spectrograph and Imager for Keck Observatory", SPIE proceedings \_\_\_\_\_ Kona 1998
- 2) Hilyard, D. Chemical Reactivity Testing of Optical Fluids and Materials in the DEIMOS Spectrographic Camera for the Keck II Telescope
- 3) Ahmed Anees, " Handbook of Opto-mechanical Engineering", 1997 CRC press NY
- 4) Vukobratovich, Daniel, "Introduction to Optomechanical Design", course notes



5) Paul R. Yoder, "Opto-Mechanical Systems Design", 1993 Marcel Dekker inc, NY NY